Smart Mater. Struct. **18** (2009) 125013 (4pp) doi:10.1088/0964-1726/18/12/125013

A simple route to synthesize $ZnFe_2O_4$ hollow spheres and their magnetorheological characteristics

Wanquan Jiang[1,3], Zhen Cao[1], Rui Gu[2], Xingzhu Ye[2], Cuifeng Jiang[1] and Xinglong Gong[2,3]

[1] Department of Chemistry, USTC, Hefei 230026, People's Republic of China
[2] CAS Key Laboratory of Mechanical Behavior and Design of Materials, Department of Modern Mechanics, USTC, Hefei 230027, People's Republic of China

E-mail: jiangwq@ustc.edu.cn and gongxl@ustc.edu.cn

Received 3 July 2009, in final form 3 September 2009
Published 6 October 2009
Online at stacks.iop.org/SMS/18/125013

Abstract
In this paper, a simple route to synthesize hollow spheres of $ZnFe_2O_4$ without the assistance of a template is reported. The crystal structure and morphology of these particles were characterized by x-ray diffraction (XRD), transmission electron microscopy (TEM), and field emission scanning electron microscopy (FE-SEM). It was found that the final products were hollow spheres with perfect morphology, and their size and the thickness of their shells decreased with the increase of urea precursor. Ferromagnetism was observed from the magnetic hysteresis loops of the $ZnFe_2O_4$ hollow spheres at room temperature. The possible formation mechanism of the hollow spheres is discussed. In addition, $ZnFe_2O_4$ magnetorheological (MR) fluids were prepared and then their MR effect was investigated on a rotational rheometer equipped with a magnetic field generator.

1. Introduction

Magnetorheological (MR) fluids, discovered by Rabinow in 1948, are a type of newly developed intelligent material [1]. MR fluids are generally suspensions of magnetic particles dispersed in nonmagnetic liquid carriers [2]. Under the application of magnetic field, MR fluids rapidly transform from a liquid-like to solid-like state so that their rheological properties, such as an enhanced shear stress, appear. Once the magnetic field withdraws, MR fluids will recover their original state in several milliseconds. Because of the quick and adjustable MR effect of MR fluids, they are widely used in shock absorbers, clutches, hydraulic valves, polishing devices, etc [3, 4].

Water is usually used as matrix in MR polishing due to its low cost, non-toxicity, good lubricity, and high polishing effect [5]. However, the problem is subsidence stability, because the classical magnetic particles have high density and they easily settle due to gravity. Therefore, hollow spheres are expected to increase the stability of suspensions when compared with their solid counterparts [6]. Although much work has been reported on the synthesis of nanosized zinc ferrites, the successful synthesis of $ZnFe_2O_4$ with attractive morphology is limited [7, 8]. Classical methods of synthesizing magnetic hollow spheres are mainly based on layer-by-layer adsorption of magnetic particles onto hard templates, and the further removal of the core either with the addition of a solvent or high temperature [9, 10]; these methods are tedious and time-consuming.

In this paper, magnetic hollow spheres of $ZnFe_2O_4$ in an EG system were prepared by an improved solvothermal method [11, 12]. This method can not only obtain hollow spheres through the one-step solvothermal route, but also avoid the use of additional templates and high temperatures during the reaction. Furthermore, a possible formation mechanism of the hollow spheres and the MR effect of water-based MR fluids were simply discussed.

2. Experimental details

2.1. Synthesis of $ZnFe_2O_4$

Analytical grade zinc chloride ($ZnCl_2$), ferric chloride hexahydrate ($FeCl_3$), urea, and ethylene glycol (EG) and

[3] Authors to whom any correspondence should be addressed.

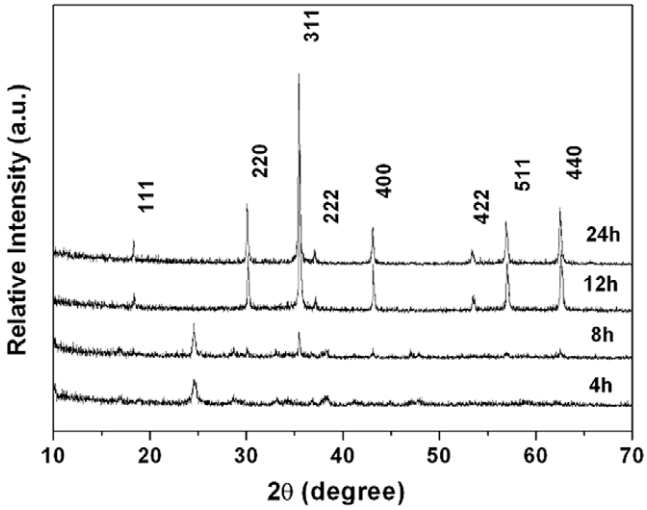

Figure 1. XRD patterns of samples prepared at different reaction times.

chemically pure polyethylene glycol 600(PEG-600) were used. All reagents were purchased from Shanghai Chemical Reagents Company in China and used directly without any further processing.

In a typical experimental procedure for the preparation of $ZnFe_2O_4$ hollow spheres, stoichiometric amounts of $FeCl_3{\cdot}6H_2O$ (5 mmol) and $ZnCl_2$ (2.5 mmol) were dissolved into 40 ml EG solvent, adding 1.0 ml PEG-600 drop by drop as stabilized reagent. Then 45 mmol urea was added slowly under stirring, keeping on stirring for about 20 min, and a homogeneous suspension was obtained. The mixture was sealed in a Teflon-lined stainless-steel autoclave (45 ml capacity) and maintained at 200 °C for 24 h in an oven. After being cooled to room temperature naturally, the obtained black products were washed several times with distilled water and absolute ethanol, and then dried in vacuum at 50 °C for 12 h.

MR fluids were prepared by dispersing the samples directly into distilled water, and the particles volume fraction was about 30%.

2.2. Characterization

X-ray diffraction (XRD) patterns were recorded on a Philips Xpert diffractometer with Cu Kα radiation (λ = 0.151 478 nm) at a scanning rate of 0.02° s^{-1} in the range of 2θ = 10°–70°. The morphology of the samples was investigated by scanning electron microscopy (SEM, Sirion 200). Crystallite size was carried on a transmission electron microscope (TEM, Hitachi H-800) with an accelerating voltage of 200 kV. The powders were dispersed in ethanol by sonication, and a drop was dripped on a supported copper grid. The magnetic properties were measured on a vibrating sample magnetometer (PPMS-9T). MR characteristics were investigated using a rotational rheometer (Physica, MCR 301, Anton Paar, Austria) with the magnetorheological device at 25 °C for all the tests. A parallel-plate measuring system (PP20) with a diameter of 20 mm was used at a gap of 1 mm.

3. Results and discussion

3.1. Characteristics and mechanism

Typical synthesis of $ZnFe_2O_4$ nanocrystal was carried out in a solvothermal system by a coprecipitation reaction between $FeCl_3$ and $ZnCl_2$. The crystalline structure was characterized by XRD. As shown in figure 1 (24 h), the reflection peaks can be easily indexed as cubic system $ZnFe_2O_4$ with cell parameter of a = 8.404 Å which is consistent with the reported value (JCPDS 01-1109, a = 8.403 Å). No obvious impurity phase was detected.

Representative TEM and SEM images of the samples prepared with processed urea under a reaction time of 24 h (shown in figure 2) were obtained by a typical preparation process. In our system, the urea was processed previously to obtain ultrafine and uniform microcrystals. It is worth noting that the sample was composed of a large number of hollow spheres and they dispersed well. In addition, the as-synthesized $ZnFe_2O_4$ spheres were single-crystalline based on the ED characterization.

In order to investigate the formation mechanism of hollow $ZnFe_2O_4$, a series of experiments were designed. Figures 1 and 3 are the typical XRD patterns and TEM images of the samples prepared at different reaction times, respectively. From the XRD patterns one can see that the samples with reaction times of 12 and 24 h exhibited identical face-centered cubic spinel structures of $ZnFe_2O_4$. However, when the reaction time was less than 12 h, the products became impure.

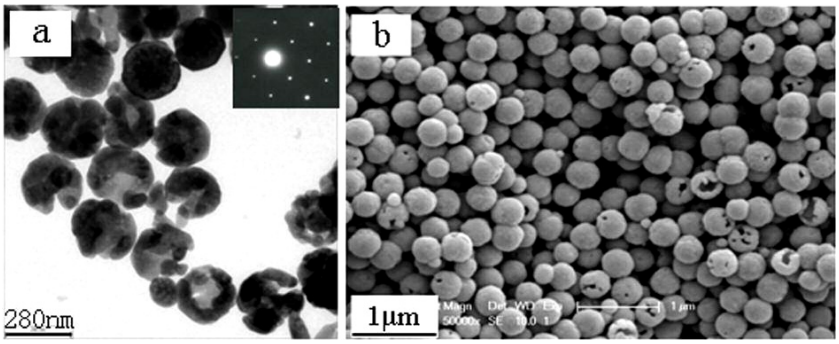

Figure 2. (a) TEM and (b) SEM images of nanoparticles prepared with processed urea under the reaction time of 24 h, the inset is the ED of a hollow sphere.

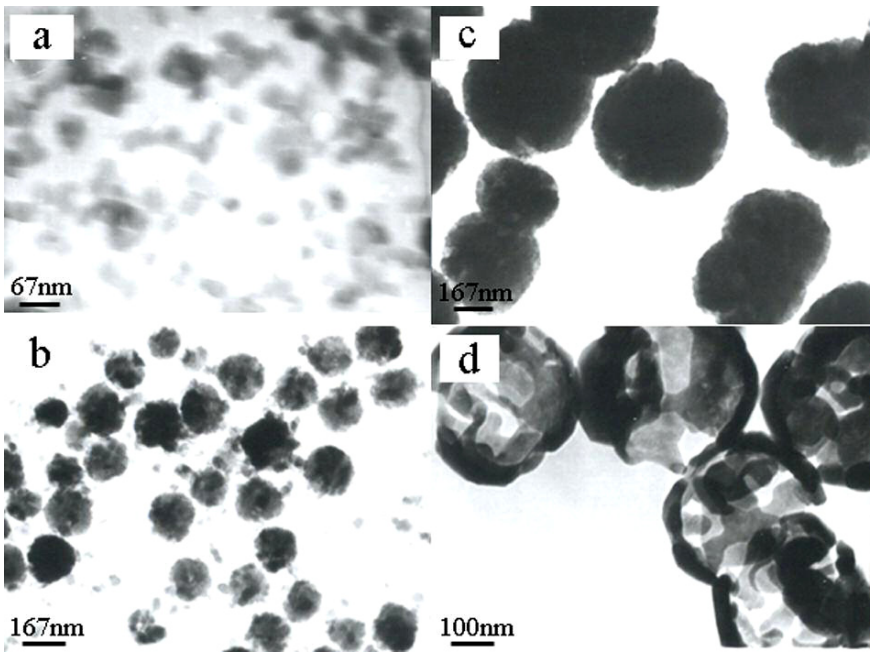

Figure 3. TEM images of samples prepared at different reaction times of (a) 4 h, (b) 8 h, (c) 12 h, (d) 24 h, respectively.

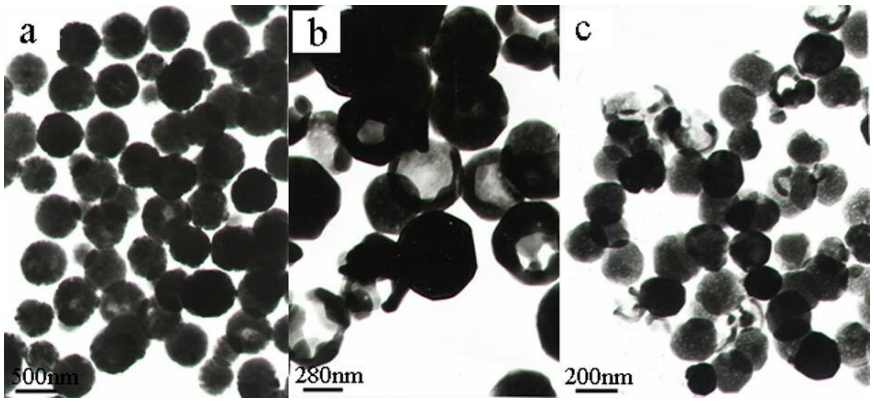

Figure 4. TEM images of samples prepared using different amounts of urea: Fe^{3+}/urea; (a) 1:5, (b) 1:9, (c) 1:11.

The reason was that the formation of $ZnFe_2O_4$ hollow spheres needed a certain time. As we know, urea can decompose thermally at a relatively low temperature (below 100 °C) while releasing a high volume of gas and increasing the pH of the solution, thereby promoting the precipitation of the metals as oxy/hydroxides. A further annealing of these intermediates promotes their conversion into the desired metal oxides. The typical reactions of preparing $ZnFe_2O_4$ are as follows:

$$CO(NH_2)_2 + 3H_2O \rightarrow CO_2 + 2NH_4^+ + 2OH^- \quad (1)$$

$$2Fe^{3+} + Zn^{2+} + 8OH^- \rightarrow ZnFe_2O_4 + 4H_2O. \quad (2)$$

The rate of the reaction (2) was slow and it took a relatively long time to complete the experiment, therefore, nonmagnetic mixtures of these metal oxy/hydroxides were obtained when the time was not long enough (figure 1 8 h and figure 3(b)). In this system urea existed in the form of microcrystals, Fe^{3+}, Fe^{2+}, and OH^- lost some energy owing to the collisions on the surface of urea microcrystals and formed $ZnFe_2O_4$, then they further grew up onto the surface, and the release of gas resulted in the formation of hollow structures.

At the same time, the influence of dosage of precursor urea on the morphology of $ZnFe_2O_4$ was also studied. Figures 4(a)–(c) show the TEM images of the sample produced using different amounts of urea while keeping other conditions constant. It can be clearly observed that the particle size decreased from 400 to 130 nm with the increase of the amounts of urea, because the urea could act as the center of heterogeneous nucleation. This result is in accordance with the classical theories of crystal heterogeneous nucleation, and it further confirmed the formation mechanism discussed above.

The magnetic hysteresis loops of the $ZnFe_2O_4$ sample (figure 5) exhibited ferromagnetic properties with saturated magnetization (M_s), remnant magnetization (M_r), and coercivity (H_c) values of 83.4 emu g^{-1}, 8.78 emu g^{-1}, and 62.6 Oe, respectively. The relatively high M_s was induced by the superexchange effect. In this solvothermal system, partial Fe^{3+} were induced into Fe^{2+}, which would produce iron–zinc

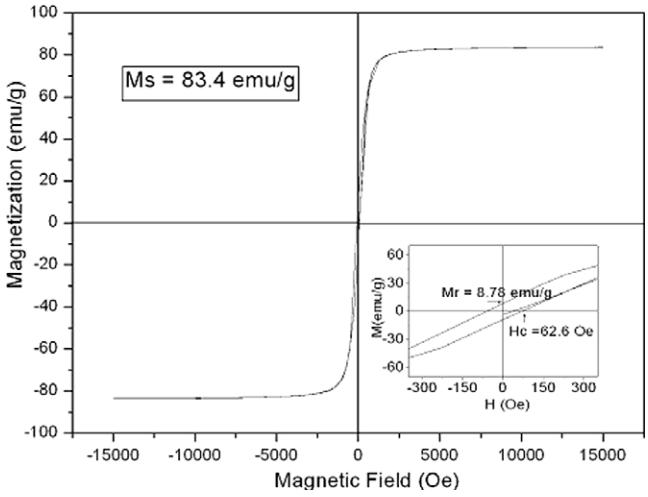

Figure 5. Magnetic hysteresis curve (M–H) of prepared $ZnFe_2O_4$ at room temperature. The inset is the enlargement of the center part of the curve.

ferrite $Zn_xFe_{3-x}O_4$, therefore the Fe^{3+} in the interspaces of the tetrahedron was partially substituted by antimagnetic Zn^{2+}, and the superexchange effect which existed in the site of Zn–O–Fe resulted in the high saturation magnetization.

3.2. Magnetorheological characteristics

To study the rheological characteristics of $ZnFe_2O_4$ MR, the magnetic flux density sweep was measured and the flow curves are shown in figures 6(a) and (b), respectively. It can be seen from figure 6(a) that the shear stress increased quickly when the magnetic flux density was small. However, it increased slowly when the magnetic flux density was bigger than 0.2 T because of the saturation of magnetic particles. The shear stress can increase from 0.2 kPa to nearly 11 kPa with the magnetic flux density swept from 0.005 to 1 T. This result exhibited the excellent MR effect of $ZnFe_2O_4$ MR fluids. Furthermore, figure 6(b) showed that the shear stress was insensitive to shear rate with the shear rate ranged from 1 to 100 s^{-1}, and the shear stress increased obviously when the magnetic flux density increased. The relation between shear stress and shear rate can be described well by the Bingham plastic model.

4. Conclusions

In summary, novel zinc ferrite spheres with hollow structure have been fabricated by a one-pot solvothermal method. The reason for the formation of the hollow structure is that the $ZnFe_2O_4$ deposition grew up on the surface of urea which further decomposes into CO_2 and NH_3. By controlling the amount of urea and the reaction time, the size and ratio of the hollow spheres can be adjusted. The $ZnFe_2O_4$ particles prepared in the present way showed good dispersion, low density, and high saturation magnetization. In addition, the water-based MR exhibited excellent stability and MR effect, which may have potential applications in polishing and biomedical fields.

Acknowledgments

The financial support from NSFC (Grant No 10672154) and SRFDP of China (Project No 20050358010) is gratefully acknowledged. The scholarship BRJH funding of the Chinese Academy of Science is also appreciated.

References

[1] Rabinow J 1948 *AIEE. Trans.* **67** 1308
[2] Bica J 2006 *J. Magn. Magn. Mater.* **299** 412
[3] Choi H J, Park B J, Cho M S and You J L 2007 *J. Magn. Magn. Mater.* **310** 2835
[4] Hynninen A P and Dijkstra M 2005 *Phys. Rev. Lett.* **94** 138303
[5] Kordonski W and Jacobs S 1996 *J. Intell. Mater. Syst. Struct.* **7** 131
[6] Zhang Y Q, Huang Z B, Tang F Q and Ren J 2006 *Thin Solid Films* **515** 2555
[7] Zhao J A, Mi L W, Hou H W, Shi X J and Fan Y T 2007 *Mater. Lett.* **61** 4196
[8] Hofmann M, Campbell S J, Ehrhardt H and Feyerherm R 2004 *J. Mater. Sci.* **39** 5057
[9] Caruso F, Spasova M, Susha A, Giersig M and Caruso R A 2001 *Chem. Mater.* **13** 109
[10] Zhu Y H, Da H, Yang X L and Hu Y 2003 *Colloids Surf.* A **231** 123
[11] Deng H, Li X L, Peng Q, Wang X, Chen J P and Li Y D 2005 *Angew. Chem. Int. Edn* **44** 2782
[12] Chen X Y, Zhang Z J, Li X X and Shi C W 2006 *Chem. Phys. Lett.* **422** 294

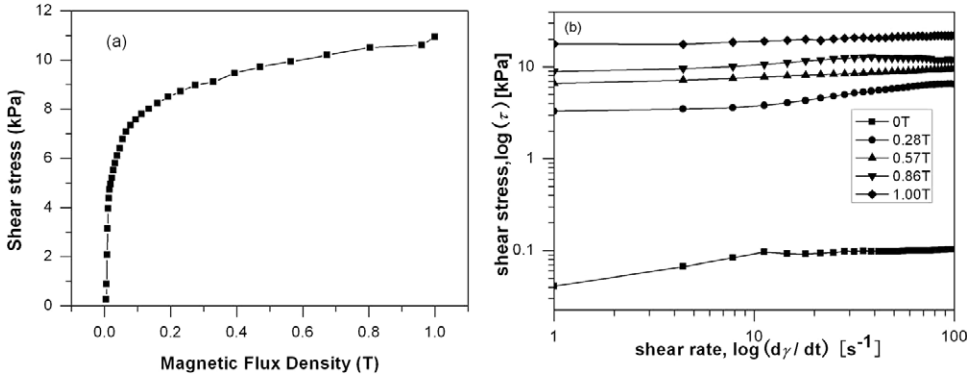

Figure 6. (a) Shear stress as a function of magnetic flux density at $\gamma = 10^{-1}$ and (b) the flow curves under different magnetic flux density.